Conformational analysis of symmetric bilirubin analogues with varying length alkanoic acids. Enantioselectivity by human serum albumin

Francesc R. Trull,*[,a] Richard V. Person[b] and David A. Lightner*[,b]

[a] *Departament de Química Orgànica, Facultat de Química, Universitat de Barcelona, C/Martí i Franquès 1, E-08028, Barcelona, Catalunya, Spain*
[b] *Department of Chemistry, University of Nevada, Reno, Nevada, 89557-0020, USA*

Symmetric analogues of mesobilirubin-XIIIα, with propionic acid groups shortened to acetic and lengthened to undecanoic, exhibit induced circular dichroism (ICD) in pH 7.5 buffered aqueous [1–5% dimethyl sulfoxide (DMSO) co-solvent] solution in the presence of human serum albumin (HSA). The CD spectra exhibit bisignate Cotton effects with $\Delta\varepsilon^{max}_{434} = +87$, $\Delta\varepsilon^{max}_{389} = -54$ (acetic), $\Delta\varepsilon^{max}_{436} = +37$, $\Delta\varepsilon^{max}_{388} = -42$ (propionic), $\Delta\varepsilon^{max}_{420} = -15$, $\Delta\varepsilon^{max}_{370} = +8$ (butyric), [$\Delta\varepsilon^{max}_{433} = -97$, $\Delta\varepsilon^{max}_{388} = +89$ in 30% aqueous DMSO], $\Delta\varepsilon^{max}_{449} = +6$, $\Delta\varepsilon^{max}_{397} = -46$ (valeric), $\Delta\varepsilon^{max}_{440} = +57$, $\Delta\varepsilon^{max}_{392} = -96$ (caproic), $\Delta\varepsilon^{max}_{440} = +15$, $\Delta\varepsilon^{max}_{393} = -21$ (caprylic) and $\Delta\varepsilon^{max}_{448} = +18$, $\Delta\varepsilon^{max}_{385} = -31$ (undecanoic). These values result from chromophore conformation (*i.e.* exciton coupling) and enantioselectivity by the protein (*i.e.* preference for a given bilirubin enantiomer). The UV–VIS spectra of the acetic to butyric, caprylic and undecanoic complexes are similar in shape, with a shoulder in addition to the main band, and reminiscent of that of the bilirubin-IXα HSA complex, indicating an analogous, folded conformation for all. The spectra of the valeric and caproic complexes, in turn, are more symmetric and red-shifted, suggesting a more extended conformation. Experimental CD values in each of these two series have been interpreted in terms of the different enantioselectivity by the protein, with the right handed acetic and caproic enantiomers fitting best the protein binding site ($\Delta\Delta\varepsilon$ *ca.* 150) and the protein showing a lower preference for the right handed propionic enantiomer ($\Delta\Delta\varepsilon$ *ca.* 80) and even lower for the right handed valeric, caprylic and undecanoic enantiomer ($\Delta\Delta\varepsilon$ *ca.* 50), but left handed butyric enantiomer ($\Delta\Delta\varepsilon$ *ca.* 24).

The differences observed in the UV–VIS spectra of each complexed (in aqueous buffer) *vs.* uncomplexed pigment (in MeOH), *i.e.* spectral shifts (7–11 nm for acetic to butyric and undecanoic, 12 nm for valeric and 16–18 nm for caproic and caprylic) and shape (reduction from two to one transition for valeric and caproic—but not for the rest) reflect the changes in pigment conformation induced by the protein. These changes are especially noticeable for the caproic and caprylic analogues.

Taken collectively, the present results indicate that the length of the alkanoic acid chains at C8 and C12 is essential for determining not only the pigment conformation, but also the enantioselectivity by the protein (through specific pigment–protein interactions) and agree with previous suggestions that these interactions may involve (at least) one salt linkage and hydrogen bonding.

The effect upon the ICD of each rubin-HSA complex of other parameters such as the percentage of DMSO used as carrier in the solution and the nature of the buffer has also been investigated. Surprisingly, an increase in the amount of DMSO from 3–30% results in dramatic changes in the observed CD of the butyric and (to a lesser extent) propionic, undecanoic complexes. These have been interpreted in terms of selective changes in the tertiary structure of the protein.

Introduction

Bilirubin-IXα (BR), **1**, is the pigment of jaundice.[1] In aqueous base and in a number of organic solvents, it is known to exist as a mixture of two folded three-dimensional conformations which are stabilized by six intramolecular hydrogen bonds between the propanoic acid carboxy groups at C8 and C12 and the opposing dipyrrinone lactam and pyrrole NH–C=O groups (Fig. 1).[2] These two conformations are non-superimposable mirror-images, and for **1** the interconversion rate of the conformational enantiomers is known to be fairly rapid at room temperature.[3,4] This hydrogen-bonded 'ridge-tile' structure has also been confirmed in the crystal.[5]

Bilirubin-IXα binds tightly to human serum albumin (HSA; K_{assoc} *ca.* 10^8 dm^3 mol^{-1} at physiological pH) at apparently only the high affinity site, forming a 1 : 1 association complex.[6,7] The proclivity of bilirubin to form association complexes with serum albumin and other proteins[6–10] is one of the properties that dominate the transport and metabolism of the pigment *in vivo*.[6,8,10,11] The human serum albumin (HSA) complex of **1** shows an induced CD for the bound pigment. The CD spectrum of a *ca.* 2.5×10^{-5} M solution of **1** in pH 7.4 argon-saturated 0.05 M aqueous Tris buffer in the presence of *ca.* 5.0×10^{-5} M HSA at 22 °C is characterized by two oppositely signed Cotton effects, at 460 nm ($\Delta\varepsilon$ +50) and 407 nm ($\Delta\varepsilon$ −25). These are derived from an exciton splitting mechanism,[12] and are interpreted in terms of a preferential binding by the protein of the pigment *P*-chirality conformational enantiomer.[13] In an attempt to elucidate the factors governing the pigment to protein interaction in this complex, the induced circular dichroism (ICD) spectra of a number of bilirubin-IXα albumin complexes have been investigated.[13–17] These conformational studies indicate that, in the presence of HSA (or bovine serum albumin, BSA), **1** always shows bisignate CD Cotton effects in the region of the pigment's long wavelength, the actual values depending on a number of variables, including the ratio of **1** to protein, pH and presence of electrolytes. In light of these results, in the presence of HSA at physiological pH, **1** is taken as also existing in a 'ridge-tile' type of conformation, with the two dipyrrinone units interacting to give the characteristic exciton coupling and

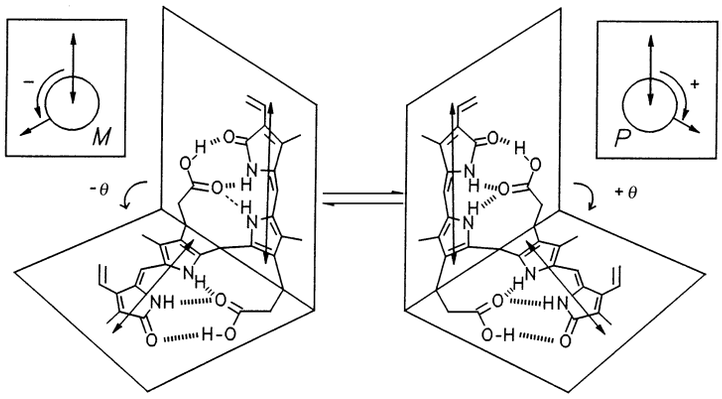

Fig. 1 Interconverting intramolecularly hydrogen-bonded enantiomeric conformers of bilirubin-IXα. The double headed arrows represent the dipyrrinone long wavelength electric transition moment vectors (dipoles) associated with the UV–VIS spectrum of the pigment. The relative helicities (*M*, minus or *P*, plus) of the vectors are shown (inset) for each enantiomer. Theta (θ) is the fold angle or the dihedral angle at the intersection of the planes containing each of the two dipyrrinones. Hydrogen bonds are represented by dashed lines.

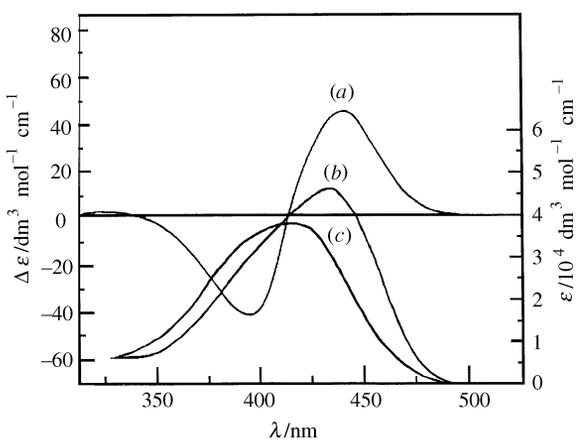

Fig. 2 Induced circular dichroism (*a*) and UV–VIS (*b*) spectra of *ca.* 2.5×10^{-5} M mesobilirubin-XIIIα on human serum albumin (*ca.* 5.0×10^{-5} M) in pH 7.4 aqueous Tris buffer at 22°. (*c*) UV–VIS spectrum of the same concentration of MBR-XIIIα without added HSA. The corresponding CD spectrum falls on the $\Delta\varepsilon = 0$ line.

the protein binding preferentially to the right handed (chiral) enantiomer—left handed in BSA. For the **1**–HSA complex, a binding model has been proposed where at least one salt linkage plays a major role in the enantioselectivity by the protein of the folded conformation stabilized by inter- and intra-molecular hydrogen bonds.[14] In this particular case, the pigment to protein interaction apparently does not substantially modify the conformation of bilirubin—relative to the one of the free pigment in solution; rather, it is the protein which adapts to the preferred bilirubin conformation. It has recently been reported that enzyme activity and enantioselectivity are directly related to protein flexibility.[18] In other studies from resonance CARS spectroscopy of the bilirubin-IXα-HSA complex, there is indication of interaction between the lactam oxygens and protonated amino groups.[19]

Under essentially the same conditions, the CD spectrum of a mesobilirubin (MBR-XIIIα)-HSA complex (Fig. 2) is similar to that of **1**, with Cotton effects at 440 nm ($\Delta\varepsilon$ +45) and 395 nm ($\Delta\varepsilon$ −40). These results indicate an analogous conformation for the two pigments and a preferential binding of the pigment *P*-chirality conformational enantiomer for both pigments.

In contrast, bilirubins and analogues that cannot adopt the folded, hydrogen-bonded conformation; *i.e.* MBR-IVα, xanthobilirubic acid, *etc.* show only monosignate ICD Cotton effects under the same conditions.[13] In addition, the CD spectra of bilirubin esters, including the dimethyl esters of **1**, MBR-XIIIα and MBR-IVα and of other bilirubins without acid groups, such as etiobilirubin-IVγ, show much weaker Cotton effects under the same conditions; *i.e.* $\Delta\varepsilon^{max}_{470} = +0.5$, $\Delta\varepsilon^{max}_{420} = -2$ for the dimethyl ester of **1**, suggesting a much smaller enantioselectivity by the protein for a positive chirality in this case.[14]

In order to explore the importance of the length of the two alkanoic acid groups at C8 and C12 on the 3D-conformation in solution, we recently used chiral sulfoxides for studies of solvent-induced CD spectra of a number of MBR-XIIIα analogues where both propionic acid groups were replaced with shorter or longer chain alkanoic acids.[20] In that study and the current work we refer to the MBR-XIIIα analogue with two acetic acid groups as MBR ($n = 1$), that with two butyric acid groups as MBR ($n = 3$), *etc.*

The work using chiral sulfoxides clearly indicated that the length of the alkanoic acid groups is essential in determining the conformation of the pigment–sulfoxide complex; in particular, propionic acid groups were shown to have a unique ability to determine a conformation with a bisignate ICD opposite in sign to those of all other analogues studied.

Similarly, if at least one salt linkage and both inter- and intra-molecular hydrogen bonding are involved in the binding of bilirubin to HSA,[14] one would expect that substitution of the two propionic acid groups at C8 and C12 by shorter and longer chain alkanoic acids should result in different bilirubin–protein binding abilities.

In the present paper, the effect of gradual lengthening (from acetic to undecanoic) of the alkanoic chains present in the pigment upon some of the stereochemical properties of the complexes with human serum albumin is discussed; in particular, with respect to: (*i*) the retention of hydrogen bonding along the series of analogues; (*ii*) how such hydrogen bonding might affect the shape of the pigment; and (*iii*) how sensitive the enantioselectivity by human serum albumin is to alkanoic acid chain length. The work is important because it shows that the length of the alkanoic acid chains at C8 and C12 is essential in determining both the shape of the pigment and the enantioselectivity by the protein.

Experimental

All circular dichroism (CD) spectra were recorded on a JASCO J600 spectropolarimeter, and all UV–VIS spectra were run on a CARY 219 spectrophotometer. Both types of spectra were run in a 1 cm rectangular cell; a solution of exactly the same pigment concentration but lacking the protein was used to record the baseline in CD; a solution of the same protein concentration but lacking the pigment was used as baseline in the UV–VIS spectra. NMR spectra were determined on a GE QE-300 300 MHz spectrometer in $CDCl_3$ solvent and are reported in δ ppm downfield from $SiMe_4$, with *J* values in Hz. Melting points were determined on a Mel-Temp capillary apparatus and are uncorrected. Combustion analyses were carried out by Desert Analytics, Tucson, AZ. Analytical TLC was carried out

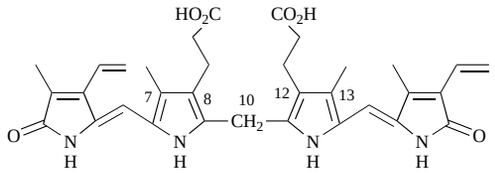

Bilirubin-IXα

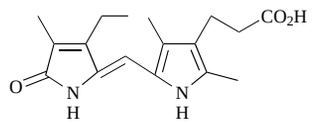

Xanthobilirubic Acid

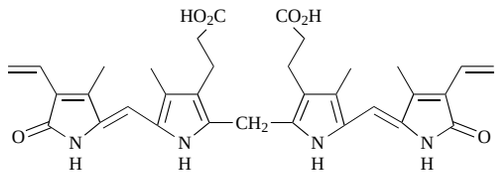

Bilirubin-IIIα

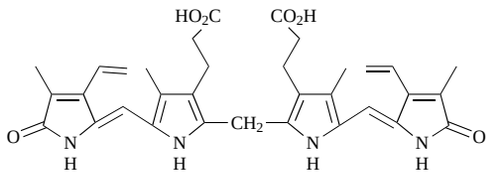

Bilirubin-XIIIα

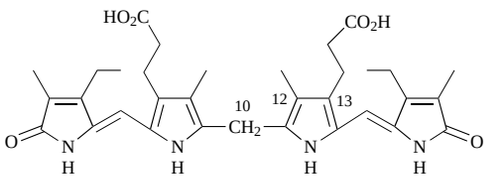

Mesobilirubin IVα

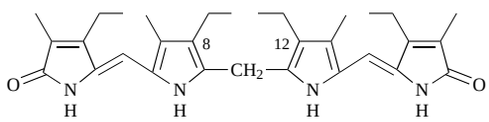

Etiobilirubin-IVγ

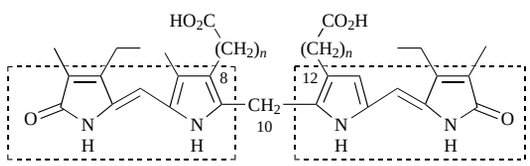

Dipyrrinone Dipyrrinone

Mesobilirubin-XIIIα Analogues
(n = 1 – 5, 7 and 10)
(n = 2) is Mesobilirubin-XIIIα

on J. T. Baker silica gel IB-F plates (125 μm layers). Flash column chromatography was carried out using Woelm silica gel F, TLC grade. HPLC analyses were carried out on a Perkin-Elmer Series 4 high performance liquid chromatograph, with an LC-95 UV–VIS spectrophotometric detector (set at 410 nm) equipped with a Beckman-Altex ultrasphere-IP 5 mm C-18 ODS column (25 × 0.46 cm) and a Beckman ODS precolumn (4.5 × 0.46 cm). The flow rate was 1.0 cm^3 min^{-1} and the elution solvent was 0.1 M dioctylamine acetate in 5% aqueous methanol (pH 7.7, 31 °C). Bilirubin-IXα (Porphyrin Products) was purified as described previously.[10] Its symmetrical isomers bilirubin-IIIα and bilirubin-XIIIα were synthesized as previously reported[21–23] as were the corresponding mesobilirubins and etiobilirubin-IVγ.[24,25]

The mesobilirubin-XIIIα (n = 1) to (n = 5) analogues reported in this work were prepared by total synthesis as described earlier,[26] as has been the (n = 10)[27] analogue. The synthesis of the (n = 7) analogue is described below. Defatted human serum albumin and Trizma buffer were obtained from Sigma Chemical Co. The phosphate buffer, pH 7.4, was 0.0096 M in KH_2PO_4 and 0.0297 M in K_2HPO_4. The mesobilirubin HSA solutions were prepared using dimethyl sulfoxide (DMSO) as carrier (final concentration, *ca.* 1%, except when otherwise noted), as previously reported for bilirubin IXα-albumin.[14] The final pigment concentration was *ca.* 2.5×10^{-5} M, giving a pigment : albumin mole ratio of *ca.* 1 : 2. The pH was measured at 22 °C on a microprocessor pH/millivolt meter (Model 811, Orion Research, Inc., Boston MA). Conformational energy maps for the molecular modelling of the pigments of this work follow from molecular mechanics calculations carried out on an Evans and Sutherland ESV-10 workstation using version 5.5 of SYBYL (Tripos Assoc., St. Louis, MO).[2,27] The dipyrrinone units of each mesobilirubin-XIIIα analogue were rotated independently about the central $-CH_2-$ at C10 (torsion angles φ_1 and φ_2) through 10° increments from 0° to 360°. (The $\varphi_1 = 0°$, $\varphi_2 = 0°$ conformer has a porphyrin shape.) In this procedure,[2] the two torsion angles were held fixed at each increment while the remainder of the molecule was relaxed to its minimum energy conformation using molecular mechanics. This was followed by a molecular dynamics cooling curve consisting of the following temperatures and times: 100 fs at 20 K, 100 fs at 10 K, 100 fs at 5 K, 200 fs at 2 K, 200 fs at 1 K, 200 fs at 0.5 K, 300 fs at 0.1 K. This was followed by molecular mechanics minimization, which gave the lowest energy conformation for each set of φ values.

3-Ethyl-8-(7-methoxycarbonylheptanoyl)-2,7,9-trimethyldipyrrin-1(10*H*)-one methyl ester

Aluminium chloride (0.52 g, 4.0 mmol) was suspended in 1,1,2,2-tetrachloroethane (15 cm^3) in a 25 cm^3 three-neck round-bottomed flask. Methyl suberoyl† chloride (from Aldrich, 0.42 g, 2.0 mmol) was added to the flask and stirred at room temperature for 30 min. 3-Ethyl-2,7,9-trimethyldipyrrin-1(8*H*,10*H*)-one (0.23 g, 1.0 mmol) was added to the flask and stirred at 60 °C for 2 days [monitored by TLC, silica, eluent: CH_2Cl_2–CH_3OH (20 : 1), R_f 0.50 and 0.75]. The reaction mixture was cooled, taken up in CH_2Cl_2 (500 cm^3), washed with water (3 × 1000 cm^3) and dried over $MgSO_4$. The solvents were evaporated and the crude product was purified by flash chromatography [TLC silica deactivated with 10% (w/w) water; eluent: CH_2Cl_2] and crystallized from CH_2Cl_2–hexane (1 : 1) to yield 0.17 g (0.42 mmol, 42%) of the pure acylated dipyrrinone. Mp 151–155 °C; $\lambda_{max}(CH_2Cl_2)$/nm 385 (ε/dm^3 mol^{-1} cm^{-1} 27 900); λ_{max}(benzene)/nm 392 (ε/dm^3 mol^{-1} cm^{-1} 32 000); ν_{max}/cm^{-1}

† Suberoyl = $-(O)C[CH_2]_6C(O)-$.

3340 (NH), 3191, 2935, 2858, 1738 (ester C=O), 1667 (ketone and lactam C=O), 1635 (C=C), 1430, 1174; δ_H($CDCl_3$, 300 MHz), 11.28 (1 H, br s, lactam −NH−), 10.62 (1 H, br s, pyrrole −NH−), 6.10 (1 H, s, =CH−), 3.69 (3 H, s, $-COOCH_3$), 2.71 (2 H, q, *J* 7.2, $-CH_2-CH_3$), 2.69 (3 H, s, C9–CH_3), 2.50 (2 H, t, *J* 7.5, $-CO-CH_2-$), 2.37 (3 H, s, C7–CH_3), 2.34 (2 H, t, *J* 7.5, $-CH_2-COO-$), 1.89 (3 H, s, C2–CH_3), 1.70, 1.40 (4 H + 4 H, 2 × m, rest of suberoyl chain), 1.17 (3 H, t, *J* 7.5, $-CH_2-CH_3$); δ_C($CDCl_3$, 300 MHz), 197.4 (ketone CO), 174.3 (ester CO), 174.1 (lactam CO), 148.6, 139.5, 128.9, 125.9, 123.6, 123.0, 122.4 (C2–C4, C6–C9), 99.8 (C5), 51.3 $COOCH_3$), 42.5, 34.0, 29.1 (2×), 24.8, 24.1 (rest of suberoyl chain), 17.8 ($-CH_2CH_3$), 15.1 ($-CH_2CH_3$), 14.8 (C9–CH_3), 12.0 (C7–CH_3), 8.5 (C2–CH_3); Found: C, 68.78; H, 8.07; N, 6.62. $C_{23}H_{32}N_2O_4$ requires C, 68.97; H, 8.05; N, 6.99%.

3-Ethyl-8-(7-methoxycarbonylheptanyl)-2,7,9-trimethyldipyrrin-1(10*H*)-one (dipyrrinone, *n* = 7)

3-Ethyl-8-(7-methoxycarbonylheptanoyl)-2,7,9-trimethyldipyrrin-1(10*H*)-one (78 mg, 0.2 mmol) in tetrahydrofuran (THF, 10 cm^3 distilled from sodium) was placed into a 25 cm^3 Erlenmeyer flask, under a nitrogen atmosphere. The flask was cooled to 0 °C and sodium borohydride (18 mg, 0.12 mmol) was added followed by addition, over 7 min, of a solution of boron trifluoride–diethyl ether (0.05 cm^3, 0.48 mmol) in THF (2 cm^3). The solution was then stirred at room temperature for 1 h. The borane was quenched with 5% aqueous HCl, and the mixture added to water (20 cm^3) and extracted with CH_2Cl_2 (2 × 20 cm^3). The extracts were dried, the solvent removed and recrystallized from CH_2Cl_2–hexane (1:1) to yield the title compound along with some residual starting material. Flash chromatography [TLC silica deactivated with 15% (w/w) water; eluent: CH_2Cl_2–CH_3OH (97:3)] afforded 70 mg (0.18 mmol, 91%) of the pure acylated dipyrrinone. Mp 112 °C (decomp.); λ_{max}(CH_2Cl_2)/nm 406 (ε/dm^3 mol^{-1} cm^{-1} 20 800); λ_{max}(CH_3OH)/nm 406 (ε/dm^3 mol^{-1} cm^{-1} 24 400); ν_{max}/cm^{-1} 3350 (NH), 3170, 2925, 2853, 1734 (ester C=O), 1683 (lactam C=O), 1628 (C=C), 1457, 1172; δ_H($CDCl_3$, 300 MHz), 11.29 (1 H, br s, lactam −NH−), 10.33 (1 H, br s, pyrrole −NH−), 6.15 (1 H, s, =CH−), 3.66 (3 H, s, $-COOCH_3$), 2.55 (2 H, q, *J* 7.5, $-CH_2-CH_3$), 2.39 (3 H, s, C7–CH_3), 2.37 (2 H, t, *J* 7.5, C8–CH_2−), 2.30 (2 H, t, *J* 7.5, $-CH_2-COO-$), 2.12 (3 H, s, C9–CH_3), 1.95 (3 H, s, C2–CH_3), 1.62, 1.43, 1.32 (2 H + 2 H + 6 H, 2 × quint. + 1 × m, *J* 7.5, rest of suberoyl chain), 1.17 (3 H, t, *J* 7.5, $-CH_2-CH_3$); δ_C($CDCl_3$, 300 MHz), 174.3 (ester CO), 174.0 (lactam CO), 148.2, 131.5, 126.8, 124.9, 122.2, 122.1, 121.4 (C2–C4, C6–C9), 101.3 (C5), 51.4 ($COOCH_3$), 34.1, 30.9, 29.3, 29.2 (2×), 25.0, 24.2 (rest of suberoyl chain), 18.0 ($-CH_2CH_3$), 15.0 ($-CH_2CH_3$), 11.7 (C9–CH_3), 9.7 (C7–CH_3), 8.5 (C2–CH_3); Found: C, 71.18; H, 8.73; N, 7.22. $C_{23}H_{34}N_2O_3$ requires C, 71.47; H, 8.87; N, 7.25%.

Mesobiliverdin-XIIIα dimethyl ester (*n* = 7)

To a solution of the foregoing dipyrrinone (*n* = 7) (70 mg, 0.18 mmol) in CH_2Cl_2 (12 cm^3) contained in a 25 cm^3 flask equipped with a magnetic stirrer and a reflux condenser was added chloranil (120 mg) and, after 5 min, formic acid (1 cm^3). The reaction mixture was refluxed in the dark, under nitrogen for 1 h. The flask was then cooled to −30 °C and the solid portion was removed by vacuum filtration. The filtrate was washed with 5% aqueous sodium hydrogencarbonate (3 × 10 cm^3) and then 5% aqueous sodium hydroxide until the washings remained basic. The organic layer was dried over $MgSO_4$ and purified by flash chromatography [TLC silica deactivated with 15% (w/w) water; eluent: CH_2Cl_2–CH_3OH (97:3)] to afford the pure verdin (68.1 mg, 0.09 mmol, 99%). The product decomposed over 100 °C; λ_{max}(CH_2Cl_2)/nm 367 (ε/dm^3 mol^{-1} cm^{-1} 29 900), 661 (15 800); ν_{max}/cm^{-1} 3200 (NH), 2931, 2854, 1700 (ester and lactam C=O), 1600 (C=C), 1100; δ_H($CDCl_3$, 300 MHz), 8.5, 7.3 (2 H + 1 H, 2 × br s, −NH−), 6.59 (1 H, s, =C10-H−), 5.89 (2 H, s, =C5,15-H−), 3.65 (6 H, s, $-COOCH_3$), 2.55 (4 H, q, *J* 7.5, $-CH_2-CH_3$), 2.47 (4 H, q, *J* 7.5, C8,12-CH_2−), 2.29 (4 H, t, *J* 7.5, $-CH_2-COO-$), 2.04 (6 H, s, C7,13-CH_3), 1.80 (6 H, s, C2,18-CH_3), 1.62, 1.52, 1.4–1.3 (4 H + 4 H + 12 H, 1 × quint. + 2 × m, *J* 7.5, rest of suberoyl chains), 1.19 (6 H, t, *J* 7.5, $-CH_2CH_3$); δ_C($CDCl_3$, 300 MHz), 174.2 (ester CO), 172.7 (lactam CO), 149.8, 146.7, 141.3, 139.8, 139.5, 128.1, 127.6, 114.0 (C2–C4, C6–C9, C11–C14, C16–C18), 96.5 (C5,10,15), 51.4 ($COOCH_3$), 34.0, 31.4, 29.2 (2×), 29.1, 24.9, 24.5 (rest of suberoyl chains), 17.8 ($-CH_2CH_3$), 14.5 ($-CH_2CH_3$), 9.6 (C7,13-CH_3), 8.3 (C2,18-CH_3); Found: C, 69.59; H, 8.37; N, 7.00. $C_{45}H_{62}N_4O_6$·H_2O requires C, 69.92; H, 8.34; N, 7.25%.

Mesobilirubin-XIIIα dimethyl ester (*n* = 7)

The foregoing mesobiliverdin-XIIIα dimethyl ester (10 mg, 0.013 mmol) was dissolved in nitrogen purged, dry propan-2-ol (5 cm^3) and methanol (0.5 cm^3). To this solution was added sodium borohydride (50 mg) and the mixture was stirred under nitrogen for one hour as it turned from blue to yellow. The suspension was acidified with 5% aqueous HCl, added to water (10 cm^3) and extracted with CH_2Cl_2. The organic layer was dried over $MgSO_4$ and the solvent removed to afford a crude yellow solid (7 mg, 0.007 mmol, 70%) that was used without further purification.

Mesobilirubin-XIIIα (*n* = 7)

To a refluxing solution of the foregoing mesobilirubin-XIIIα dimethyl ester (44 mg, 0.058 mmol) in nitrogen purged THF (6 cm^3) and methanol (1 cm^3) was added nitrogen purged 0.75 M aqueous sodium hydroxide (1 cm^3) and refluxing under nitrogen was continued for 3 h. The yellow suspension was acidified with 5% aqueous HCl and extracted with CH_2Cl_2. The organic layer was dried over $MgSO_4$ and the solvent removed to afford a red–orange residue which was dried under vacuum overnight and then purified by flash chromatography [TLC silica deactivated with 15% (w/w) water; eluent: acetone] The pure product was obtained as a yellow powder (9 mg, 0.013 mmol, 23%).

The product decomposed over 140 °C; λ_{max}(CH_2Cl_2)/nm 406 (ε/dm^3 mol^{-1} cm^{-1} 14 100), λ_{max}(CH_3OH)/nm 420 (ε/dm^3 mol^{-1} cm^{-1} 19 900); ν_{max}/cm^{-1} 3340 (NH), 2920, 2850, 1660 (acid and lactam C=O), 1630 (C=C), 1430, 1360, 1070; δ_H(CD_3SOCD_3, 300 MHz), 11.92 (2 H, br s, −COOH), 10.33 (2 H, br s, pyrrole −NH−), 9.81 (2 H, br s, lactam −NH−), 5.90 (2 H, s, =C5,15-H−), 3.86 (2 H, s, −C10-H−), 2.11 (8 H, m), 2.02 (4 H, t, *J* 7.5), 1.40 (4 H, br m), 1.20 (8 H, br m), 0.98 (8 H, m, rest of suberoyl signals + CH_2-CH_3), 1.03 (6 H, t, *J* 7.5, $-CH_2-CH_3$); δ_C(CD_3SOCD_3, 300 MHz) 174.6 (acid CO), 172.1 (lactam CO), 147.3, 130.6, 127.4, 123.1, 122.7, 121.7, 121.2 (C2–C4, C6–C9, C11–C14, C16–C18), 97.9 (C5,15), 33.9, 33.8, 29.7, 29.2, 29.0, 28.7, 24.8, 24.7 (rest of suberoyl chains + C10), 17.4 ($-CH_2CH_3$), 15.0 ($-CH_2CH_3$), 9.4 (C7,13-CH_3), 8.3 (C2,18-CH_3); Found: C, 69.95; H, 8.10; N, 7.10. $C_{43}H_{60}N_4O_6$ requires C, 70.85; H, 8.30; N, 7.69%. $C_{43}H_{60}N_4O_6$·$(CH_3)_2CO$ requires C, 70.20; H, 8.45; N, 7.12%.

Results and discussion

The UV–VIS and ICD spectra of the HSA complexes of mesobilirubins (MBRs) (*n* = 1) to (*n* = 5) in aqueous Tris buffer at *ca.* pH 7.5 are shown respectively in Figs. 3 and 4. Numerical spectral data, including MBR (*n* = 7), MBR (*n* = 10) and etiobilirubin-IVγ are given in Table 1.

It may be noted that although the CD magnitudes vary considerably, the signed order of the ICD Cotton effects remains invariant for the MBRs with *n* = 1, 2, 4, 5, 7 and 10 (and etiobilirubin-IVγ), only in the MBR (*n* = 3) is the ICD Cotton effect inverted. In this case, when the (v/v) percentage of DMSO used as carrier is increased to 30%, the ICD Cotton effect sign remains inverted but the Δε values are substantially increased (Table 3; see later).

Table 1 Relevant UV–VIS spectral data[a] in MeOH for mesobilirubin-XIIIα ($n = 1$) to ($n = 5$) analogues, and UV–VIS and induced circular dichroism in pH 7.5 aqueous Tris buffer[b] for their (1:2) pigment-HSA complexes[c,d] at 22 °C

	CD		UV–VIS ε_{max} (λ)	
Mesobilirubin-XIIIα	$\Delta\varepsilon_{max}$ (λ)	λ at $\Delta\varepsilon = 0$	1:2 Pigment:HSA (aq. buffer)	Pigment (MeOH)[e]
($n = 1$)	+87.5 (434), −54.1 (389)	406	46 600 (432), 39 700 (406)[sh]	50 200 (422), 49 800 (416), 45 600 (396)
($n = 2$)	+36.9 (436), −41.7 (388)	409	50 800 (437), 42 000 (402)[sh]	50 700 (426), 43 100 (401)
($n = 3$)	−15.5 (420), +8.2 (370)[f]	388	48 000 (437), 40 300 (406)[sh]	52 000 (428), 51 400 (415), 54 500 (398)
($n = 4$)	+6.4 (499), −46.2 (397)[g]	442	57 800 (443)	51 300 (431), 49 800 (421), 46 300 (406)
($n = 5$)	+56.6 (440), −96.3 (392)	412	55 300 (444)	54 000 (428), 51 200 (417), 50 000 (397)
($n = 7$)[h]	+15 (440), −21 (393)	414	18 400 (443), 13 800 (400)	17 600 (425), 23 400 (395)
($n = 10$)[i]	+17.9 (448), −30.9 (385)[j]		52 400 (444), 42 000 (390)[sh]	59 500 (437), 44 600 (405)
Etiobilirubin-IVγ	+3.6 (440), −5.1 (392)	409	22 900 (432), 31 300 (378)[sh]	50 000 (428), 45 000 (397)[k]

[a] $\Delta\varepsilon$ and ε in dm^3 mol^{-1} cm^{-1}; λ in nm. [b] 0.05 M Tris buffer. [c] Containing *ca.* 1% (v/v) DMSO as carrier unless otherwise indicated. [d] *Ca.* 2.5×10^{-5} M pigment, *ca.* 5.0×10^{-5} M HSA. [e] Data for MBR ($n = 1$) to ($n = 5$) from ref. 26; spectra run at 1–2 × 10^{-5} M concentrations. [f] Shoulder: −8.6 (*ca.* 400); in 30% (v/v) DMSO, the corresponding values are: $\Delta\varepsilon_{max}(\lambda) = -97$ (433), −54 (418, sh), +89 (388); $\lambda(\Delta\varepsilon = 0) = 407$; $\varepsilon_{max}(\lambda) = 42\,500$ (434), 37 500 (408). [g] Shoulder: −33.4 (*ca.* 425). [h] 3% (v/v) DMSO as carrier. [i] 5% (v/v) DMSO as carrier. [j] Shoulders: −28.9 (395), +17 (441). [k] From ref. 36.

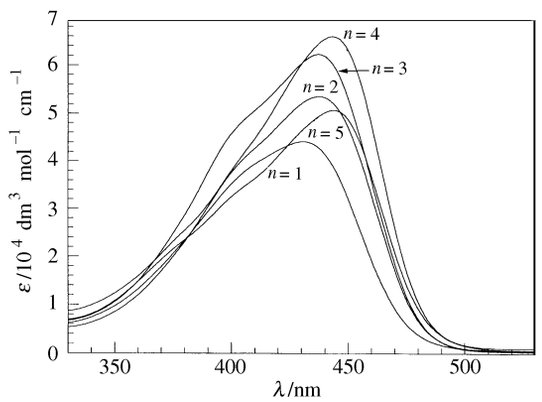

Fig. 3 UV–VIS spectra of *ca.* 2.5×10^{-5} M mesobilirubin-XIIIα ($n = 1$) to ($n = 5$) on human serum albumin (*ca.* 5.0×10^{-5} M) in pH 7.5 aqueous Tris buffer containing 1% DMSO as carrier, at 22 °C

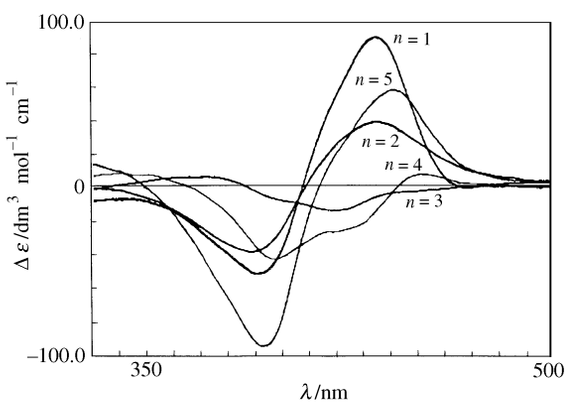

Fig. 4 Induced circular dichroism spectra of *ca.* 2.5×10^{-5} M mesobilirubin-XIIIα ($n = 1$) to ($n = 5$) on human serum albumin (*ca.* 5.0×10^{-5} M) in pH 7.5 aqueous Tris buffer containing 1% DMSO as carrier, at 22 °C

These data confirm an influence of the pigment's acid chain length on the ICD of the respective pigment–HSA complex, and it would be important to rationalize them in terms of the distinct enantioselectivity by the protein as the alkanoic chain length increases in the series. Unfortunately, there are some important limitations on the information that can be extracted from the CD spectra of bilirubin HSA complexes: binding of the two bilirubin chiral conformers to HSA results in two diastereomeric complexes, and the *P*-helicity bilirubin HSA (*P*/HSA) and the (*M*/HSA) diastereomers may have distinct spectroscopic properties. The two complexes may not only have different binding constants, but may also bind different shapes of the *M*- and *P*-helicity conformers. As a result, the magnitude of the observed Cotton effect for a given bilirubin–protein complex will be the result of the precise chromophore conformation in both the *M*- and *P*-helicity conformers; *i.e.* exciton coupling and also of the enantioselectivity by the protein; *i.e.* preference for a given bilirubin enantiomer. Therefore, conclusions about enantioselectivity in the present series of mesobilirubin-XIIIα analogues albumin complexes will only be reliable provided the ridge-tile conformations of the pigment in each complex are known (for instance, from UV–VIS spectroscopy).

For this reason, it is important that the UV–VIS spectra of the series of mesobilirubin–HSA complexes of this work be investigated in detail before an attempt is made to draw conclusions from the CD data. In this connection, we note that the conformational dependence of UV–VIS spectra has recently been applied to compute the expected absorption spectra of the bilirubin molecular exciton.[2] The results of these calculations are used in the present paper to postulate the conformations responsible for the UV–VIS spectra of each mesobilirubin-XIIIα analogue and for the UV–VIS and ICD spectra of their HSA complexes.

Conformational analysis from molecular dynamics calculations

The relative energies and stabilities of the various conformations accessible to each mesobilirubin-XIIIα analogue were assessed quantitatively using molecular mechanics force field calculations. Thus, by using molecular dynamics in the SYBYL force field program, the conformations and their energies of each bilirubin analogue were computed and displayed as three-dimensional conformational energy maps with potential energy (vertical axis) and φ_1 and φ_2 on the horizontal axes.[2b] Two of us have recently published a detailed report on the results of a similar analysis carried out on bilirubin-IXα and mesobilirubin-XIIIα ($n = 2$).[2a] Satisfyingly, for these two compounds, the SYBYL force field locates global energy minimum structures which are essentially identical to those seen in crystals of bilirubin and mesobilirubin by X-ray crystallography and very similar to the conformations computed for bilirubin or its analogues using molecular orbital calculations.[28]

In summary, two trends can be observed in this series of mesobilirubins of the current work. (*i*) While intramolecular hydrogen bonding is retained in all of the stable conformations, as the alkanoic acid chains are shortened relative to ($n = 2$); *i.e.*, for ($n = 1$), the chains have to strain more to maintain the stabilizing hydrogen bonds. This pull exhibited by the shorter chains causes the lactam ring to be twisted out of plane and moved towards the centre of the molecule. To accommodate this twisting, the two central torsion angles, φ_1 and φ_2 increase. (*ii*) As the acid chains are lengthened ($n = 2$–5 and 7), two hydrogen bonded minima within the same helicity well are observed. The general trend is that as the acid chain lengthens, the more the two minima move away from the global energy minimum of bilirubin-IXα and mesobilirubin-XIIIα ($n = 2$)

(60°, 60°) towards (0°, 0°) and (180°, 180°). Since (0°, 0°) and (180°, 180°) are energy maxima for these propellers, they can only approach (20°, 20°) and (150°, 150°) before they run into too much steric strain. Homologues with chains too long ($n = 10$) to be accommodated within this range adopt new minima that are a continuation of the previous trend, but now are forced to move around the side of the maxima at (0°, 0°) and 180°, 180°).[27]

These data show that each rubin has its own characteristic behaviour in the gas phase, in solution and probably when bound to proteins. In addition, the ability of each mesobilirubin to adopt structures differing from the theoreticaly calculated global energy minimum conformations will depend on the energy available in the system under study. Although their independent existence might be improbable, higher energy conformations might be accessible to them by association complexation, *e.g.* with proteins.

UV–VIS spectral analysis and conformation from exciton coupling

UV–VIS spectroscopy of free pigments in solution can provide important evidence about their solution conformation and, indirectly, about intramolecular hydrogen bonding; for the pigment HSA complexes, the UV–VIS spectra can give additional evidence about the pigment protein interactions.

Table 1 summarises the relevant UV–VIS data of mesobilirubin-XIIIα ($n = 1$) to ($n = 5$), ($n = 7$), ($n = 10$) and etiobilirubin-IVγ in MeOH and of their 1:2 pigment–HSA complexes in pH *ca.* 7.5 aqueous Tris buffer. The UV–VIS spectra of the ($n = 1$) to ($n = 5$) MBR–HSA complexes in pH *ca.* 7.5 aqueous Tris buffer are shown in Fig. 3.

In MeOH, a steady increase is observed in the position of the low energy absorption maximum from *ca.* 422 nm ($n = 1$) to 426 ($n = 2$), 428 ($n = 3$), 431 ($n = 4$) and 437 ($n = 10$). Exceptions to this behaviour are the ($n = 5$) and ($n = 7$) analogues, with maxima near 428 and 425 nm, respectively. Etiobilirubin absorbs near 428 nm. These changes can be interpreted in terms of the exciton coupling theory [2,29–32] (Fig. 5).

In this model, the present mesobilirubins can be seen as bichromophoric systems in which the interaction of the locally excited states of the twin dipyrrinone chromophores gives rise to the so-called exciton splitting, which generates two transitions in the UV, one higher and one lower in energy than that for the isolated dipyrrinone chromophore. This splitting is especially dependent on the magnitudes and directions of the two electronic transition moments involved and is expected to be largest for molecular geometries of the tetrapyrrole pigments where the dipyrrinone transition moments make a skew angle of *ca.* 90° (Fig. 1). There is, therefore, a correlation between the tetrapyrrole pigment conformation and its UV–VIS spectrum.[2] The component dipyrrinone chromophores of rubinoid pigments have only a small interchromophoric orbital overlap in the folded conformation (*ca.* 100° dihedral angle) of Fig. 5(*c*). As this folded conformation closes (in book-like fashion) toward the porphyrin shape [Fig. 5(*a*)], the intensity of the long wavelength UV–VIS exciton component can be expected to decrease towards zero, leaving a more symmetric, blue-shifted band.[29–31] Alternatively, as the folded conformation opens towards the linear (extended) shape [Fig. 5(*d*)], the intensity of short wavelength UV–VIS exciton component should decrease towards zero, leaving a more symmetric, red-shifted band. According to this model, the steady increase in λ_{max} observed (Table 1) in the series of MBRs ($n = 1$), ($n = 2$), ($n = 3$), ($n = 4$) and ($n = 10$) can be interpreted in terms of a concomitant opening of the folded ridge-tile conformation characteristic of the MBR ($n = 2$) analogue, towards a more extended shape. This interpretation is in contradiction with the predictions from molecular dynamics calculations (above). However, the relatively low values of the conformational interconversion barriers calculated and the fact that the calculations correspond to the unsolvated chromophores might explain this apparent inconsistency. For the MBR ($n = 1$) analogue in methanol, for instance, one could envisage a more closed conformation than predicted in the gas phase by putting the OH of methanol to act as a bridge between the acetic acid CO_2H and the lactam and pyrrole NH groups of the opposing dipyrrinone.

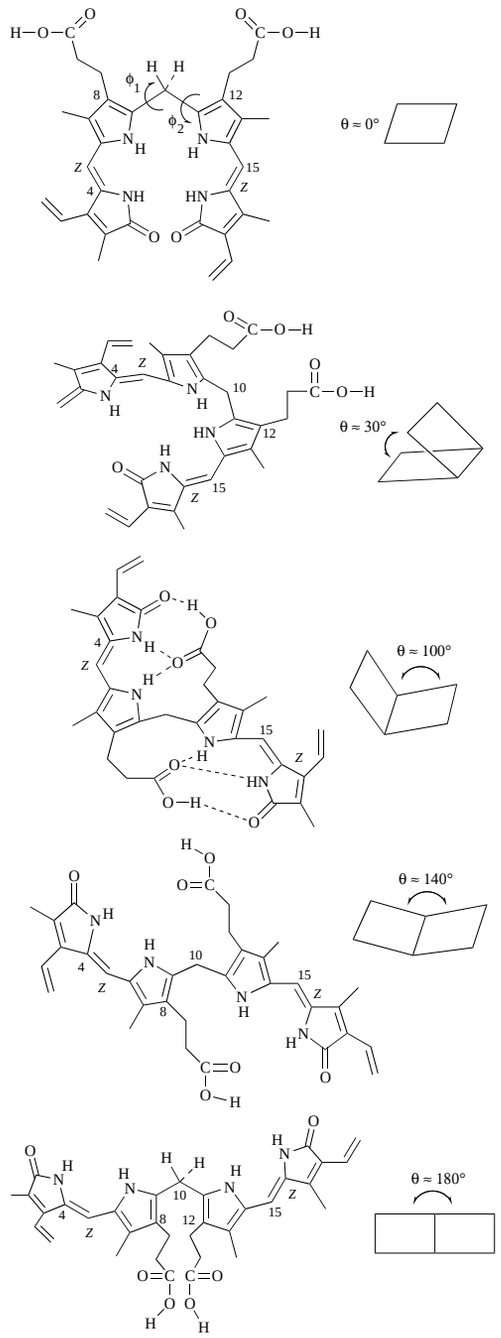

Fig. 5 Conformational drawings of representative three-dimensional structures of bilirubin-IXα. The indicated conformations are produced by rotations about the torsion angles φ_1 and φ_2 (see text), while keeping the dipyrrinone units planar. The dihedral angle (θ) of intersection of the dipyrrinone planes is represented at the right of each structure, with the line of intersection passing through C10. (*a*) The $\theta = 0°$ conformation is planar and 'helical', with both dipyrrinones lying essentially in the same plane and $\varphi_1 \approx \varphi_2 \approx 0°$. (*b*) The $\theta = 30°$ conformation is skewed and 'helical', with $\varphi_1 \approx \varphi_2 \approx 10$–$20°$. It is shown in the plus (*P*) chirality. (*c*) Folded conformations with $\theta = 90$–$110°$ and $\varphi_1 \approx \varphi_2 \approx 60$–$70°$. The ridge-tile folded structure belongs to this conformation. (*d*) The stretched conformation $\theta = 140°$, with $\varphi_1 \approx \varphi_2 \approx 130$–$170°$. The distances between the erstwhile H-bonding components are too large to accommodate the intramolecular H-bonding shown in the ridge-tile conformation. (*e*) The linear conformation, $\theta = 180°$, leads to approximate coplanarity of the dipyrrinone rings, up to $\varphi_1 \approx \varphi_2 \approx 180°$.

In addition, the small magnitude of the peak shifts and the appearance in all analogues of important shoulders in addition to the main absorption band, *i.e.* two exciton components, suggest that the corresponding conformations are in all cases deviated little from the MBR ($n = 2$) ridge-tile. According to the previous results, the effectiveness of intramolecular hydrogen bonding in the series of mesobilirubin analogues essentially increases with decreasing chain length; *i.e.* as the acid chain lengthens, the hydrogen bonding becomes weaker, exposing the carboxylic acid groups more.

These results are roughly in agreement with the distinct lipophilicity manifested by these compounds: their retention times (in min) on reverse phase HPLC[33] are 60.4 for MBR ($n = 1$), 16.3 ($n = 2$), 15.2 ($n = 3$), 15.1 ($n = 4$), 11.5 ($n = 5$), 12.0 ($n = 7$), 24.6 ($n = 10$), >120 ($n = 19$) and 10.7 (etiobilirubin-IVγ), indicating that, in the acid series, the polarity first increases in going from MBR ($n = 1$) to ($n = 5$), then decreases as the acid chain lengthens.

The UV–VIS spectra of the mesobilirubin albumin complexes in aqueous buffer (Fig. 3 and Table 1) also display a steady increase in the position of the low energy absorption maximum with increasing chain length [432 nm MBR ($n = 1$), 437 nm ($n = 2$), ($n = 3$), 443–444 nm ($n = 4$), ($n = 5$), ($n = 7$), ($n = 10$)], but this increase only takes place up to MBR ($n = 4$), ($n = 5$), with the maxima for ($n = 7$) and ($n = 10$) appearing at the same wavelength as for ($n = 4$), ($n = 5$). According to the exciton model, the increase in wavelength maximum for the MBR ($n = 1$) to ($n = 4$), ($n = 5$) complexes reflects conformations more extended as the alkanoic acid lengthens.

In addition, the spectra of the MBR ($n = 4$), ($n = 5$) complexes are unique in that they present a more symmetrical absorption band relative to the rest of members of the series (Fig. 3) in which one (or more) shoulders at lower wavelength (high energy transition) appear(s) in all cases. This unique feature of the MBR ($n = 4$), ($n = 5$) analogues is exclusive of their albumin complexes, since the spectra of the free pigments in MeOH also display shoulders (Table 1). Another particularity of the MBR ($n = 4$), ($n = 5$) [and ($n = 7$)] albumin complexes is the larger red-shifts [12 nm for ($n = 4$), 16 nm for ($n = 5$) and 18 nm for ($n = 7$)] of their low-energy absorption maxima relative to the values of the free pigments in MeOH. These larger shifts and the appearance of only one (red-shifted) band in their UV–VIS spectra [for the MBR ($n = 4$) and ($n = 5$) complexes], indicate more extended conformations for these pigment albumin complexes in aqueous buffer, relative to the free pigments in MeOH. This change in conformation must be induced by the protein. For the complexes of MBR ($n = 2$), ($n = 7$), ($n = 10$) and, to a lesser extent, ($n = 1$) the UV–VIS spectra (Fig. 3 and Table 1) show both exciton components and the two are of comparable intensity; therefore, the angle between the two transition dipole moments should be close to 90°,[2,32,34] and the pigment's conformation is probably not very different from that represented in Fig. 1. As we shall discuss later, the CD data indicate that the situation with the MBR ($n = 3$) is more intricate. In addition, for these complexes, the red-shifts, relative to the free pigments in MeOH are in the range 7–11 nm. These smaller shifts could reflect slight changes in pigment conformation due to a change in the polarity/ability to hydrogen bond of the microenvironment of the pigment in its complex with albumin—relative to MeOH. In agreement with this is the maintenance of the spectral shape for each isomer in these two environments.

Apparently, the HSA binding site can easily house mesobilirubins with shorter alkanoic acid chains, MBR ($n = 1$) and ($n = 2$), as well as those with the longer, more flexible chains ($n = 10$), all essentially in the pigment's folded solution conformations. However, for the pigments with intermediate chain lengths, MBR ($n = 4$), ($n = 5$) and ($n = 7$), which are more sterically crowded than acetic and propionic but less flexible than undecanoic, a change in conformation is required relative to that of the free pigment in MeOH before the pigments can fit into the protein binding site. As with the ($n = 3$) analogue, the CD data (below) indicate some additional phenomena with the ($n = 4$) mesobilirubin.

In summary, the conformations of mesobilirubins in MeOH and those of their albumin complexes in aqueous buffer appear to be related to the alkanoic acid chain length, probably *via* its capacity to efficiently participate in the formation of intramolecular hydrogen bonds (in the albumin complexes, also *via* its ability to intermolecular hydrogen bond and efficiently form salt linkages to the protein).

Circular dichroism and binding to albumin

The exciton coupling model is especially effective in the interpretation of CD data in terms of pigment conformation.[2,29–32,34] In the UV–VIS spectrum, the two exciton transitions have the same sign and when they are not widely separated, they show considerable overlap and result in the broad, nonsymmetric structure of the relevant UV–VIS bands (Fig. 3 and above). In the CD spectra, however, where exciton splitting leads to two transitions with oppositely signed CEs, the observed spectra (Fig. 4 and Table 1) have widely separated maxima due to considerable cancellation in the overlap region of the separated CD transitions. In this case, as the folded conformation of Fig. 1 closes towards the porphyrin shape or stretches to the extended in-line or linear conformations (Fig. 5), only one of the two exciton transitions tends to be allowed, and the orbital interaction between the chromophores can be expected to increase somewhat. Thus, the CD Cotton effects are predicted to be most intense in folded conformations [with roughly equal intensities, as in MBR ($n = 2$)] and are expected to shrink and approach zero as the porphyrin-like and linear and extended conformations are accessed. Indeed, the computed $\Delta\varepsilon$ values (Table 2) for the long wavelength transition of a number of conformations are: 0 (0°, 0°), +190 (20°, 20°), +210 (40°, 40°), +175 (60°, 60°), +120 (90°, 90°), +20 (110°, 110°), 0 (120°, 120°), *etc.*; *i.e.* highest $\Delta\varepsilon$ values for the (40°, 40°) conformation and lower $\Delta\varepsilon$ values for both the more porphyrin-like and more stretched conformations.

An additional interesting conclusion from these calculations is that the magnitude of $\Delta\varepsilon$ can also decrease and the sign of $\Delta\varepsilon$ can become inverted without an inversion of molecular chirality [for instance, the $\Delta\varepsilon$ value for the (120°, 120°) conformation is −100].[2,35] However, for bilirubin-IXα and mesobilirubin-XIIIα ($n = 2$), those conformers with inverted CD curves are computed to lie much higher in energy than the global minimum. In these cases, previously observed CD spectra with moderate or weak $\Delta\varepsilon$ values [as with bilirubin-IXα and mesobilirubin-XIIIα ($n = 2$) on human serum albumin (Fig. 2)] may be attributed to conformational changes as much as to incomplete enantioselection by the chiral complexation agent. For the mesobilirubin-XIIIα analogues of the present work, with different three-dimensional conformational energy surfaces, the contribution of protein-induced conformational changes *vs.* enantioselection to the experimentally-determined $\Delta\varepsilon$ values (Table 1) may vary from compound to compound. The HSA complexes of the present series of mesobilirubin-XIIIα analogues in aqueous buffer have bisignate CDs in all cases (Fig. 4 and Table 1), suggesting essentially folded conformations for all. This is in agreement with the conclusions from the UV–VIS data. Furthermore, the exciton model predicts the largest CE values for the MBR ($n = 3$), ($n = 4$), ($n = 5$) and ($n = 7$) analogues, and smaller values for both the higher and lower members of the series (Table 2). If we assume the computed conformation of each pigment to be the same as in its complex to HSA, which is not necessarily the case in all analogues (see above), then we should expect the highest CE values for the MBR ($n = 3$), ($n = 4$), ($n = 5$) and ($n = 7$) complexes to HSA and lower for the shorter and longer chain analogues.

Table 2 Torsion angles φ_1 and φ_2, lowest interconversion barrier and unscaled circular dichroism $\Delta\varepsilon$ for the lower energy exciton[a] corresponding to the computed minimum energy conformations of (n = 1)–(n = 5), (n = 7) and (n = 10) mesobilirubin-XIIIα analogues, from molecular dynamics[b]

Mesobilirubin-XIIIα	φ_1, φ_2	Lowest interconversion barrier/kcal mol^{-1}	Unscaled $\Delta\varepsilon$ for the lower energy exciton
(n = 1)	80°, 80°	19.7	145
(n = 2)	60°, 60°	19.5	175
(n = 3)	50°, 50°[c]	19.3	190[h]
(n = 4)	30°, 60°[d]	10.7	195[i]
(n = 5)	30°, 30°[e]	17.1	205[j]
(n = 7)	20°, 30°[f]	13.1	205[k]
(n = 10)	−70°, 50°[g]	5.0	50

[a] $\Delta\varepsilon$ values from ref. 2. [b] For additional details, see Experimental and section on Conformational Analysis. [c] The (120°, 120°) conformation lies 3.15 kcal mol^{-1} (1 cal = 4.184 J) above. [d] The (125°, 125°) conformation lies 1.0 kcal mol^{-1} above. [e] The (100°, 100°) conformation lies 8.73 kcal mol^{-1} above. [f] Long diagonal minimum energy well; the (0°, 50°) conformation lies 0.1 kcal mol^{-1} above. [g] The (60°, 180°) conformation lies 1.3 kcal mol^{-1} above. [h] $\Delta\varepsilon$ = 0 for the (120°, 120°) conformation. [i] $\Delta\varepsilon$ = −5 to −10 for the (125°, 125°) conformation. [j] $\Delta\varepsilon$ = 50 for the (100°, 100°) conformation. [k] $\Delta\varepsilon$ = 135 for the (0°, 50°) conformation.

The approximate experimental CD $\Delta\Delta\varepsilon$ values vary from 142 for MBR (n = 1) to 79 (n = 2), 24 (n = 3) [186 in 30% DMSO], 53 (n = 4) [no $\Delta\Delta\varepsilon$ value is available in 30% DMSO], 153 (n = 5), 36 (n = 7), 49 (n = 10) and 8.7 (etiobilirubin-IVγ). The major discrepancies between theoretical predictions and experimental values are found in the (n = 1) and (n = 7) analogues, although for (n = 7), the low experimental $\Delta\Delta\varepsilon$ value might be related to the low ε values of its two transitions as measured in the UV–VIS (Table 1). On the other hand, a model that explains the differences between theoretical and experimental behaviour of the (n = 1) analogue has been discussed above. In any case, the high CD $\Delta\Delta\varepsilon$ value displayed by the (n = 1) complex suggests a high enantioselectivity by the protein.

The (n = 2) complex has been the most thoroughly studied of the series. Its CD CEs have been interpreted in terms of the ridge-tile folded conformation.[13] Its UV–VIS spectrum is very similar to that of the MBR (n = 1) complex; therefore, its lower CD $\Delta\varepsilon$ values must be interpreted in terms of a lower enantioselectivity by the protein for the MBR (n = 2) pigment.

The UV–VIS spectrum of the (n = 3) complex is also similar to that of the MBR (n = 2) complex; however, at low DMSO percentages, the ICD spectra of the MBR (n = 3) [and (n = 4)] complex(es) show(s) shoulders in addition to the main peaks, probably indicating the contributions by several species. The (n = 3) rubin has a particularly odd-shaped curve which must be due to the addition of two different curves from the *M*/HSA and *P*/HSA complexes corresponding to a low enantioselectivity by the protein. The sign of the Cotton effect is opposite to that of all other members of the series, indicating a predominant enantioselectivity by the protein for the opposite conformer in this case. Less likely, the observed CD might be the result of contributions from several aggregated species.

With 30% DMSO cosolvent, the CD $\Delta\varepsilon$ values for the (n = 3) complex become much higher: −97 (433), +89 (388) and an interpretation for this observation is given below. The roughly equal (and important) intensities of the two transitions correspond to a folded conformation.

The MBR (n = 5) complex has a CD $\Delta\Delta\varepsilon$ value close to 150, the highest in the series. This result can be interpreted in terms of a higher enantioselectivity by the protein for this complex.

The CD $\Delta\Delta\varepsilon$ values for the MBR (n = 4) and (n = 10) analogues are of about one third relative to MBR (n = 5). The absorption spectra of the MBR (n = 4) and (n = 5) complexes are nearly identical; therefore, the smaller Cotton effects displayed by the MBR (n = 4) complex must correspond to a lower enantioselectivity by the protein. For the (n = 10) complex, the experimental lower CE agrees with the theoretical prediction. In this case, therefore, it is not clear whether this low CE value is the result of the particular chromophore conformation in its complex to albumin, or else it corresponds to lower enantioselectivity by the protein.

The extremely low CD $\Delta\Delta\varepsilon$ values displayed by the etiobilirubin-IVγ HSA complex, combined with a folded conformation for this pigment in the complex, from UV–VIS, must correspond to the nearly null enantioselectivity by the protein. Enantioselectivity therefore seems to require not only alkanoic acid chains in C-8 and C-12 of the pigment, but is also very sensitive to the length of these alkanoic acid chains. The present results seem to indicate that HSA is especially enantioselective for the *P* chirality conformational enantiomer of MBR (n = 1), (n = 5) and for the *M* conformation of MBR (n = 3) (in 30% DMSO). Enantioselectivity by the protein for the *P* chirality conformational enantiomer seems intermediate for the MBR (n = 2) complex, and lowest for the (n = 4) complex. The situation with the MBR (n = 7) and (n = 10) complexes is less clear.

Enantioselectivity by the protein would then be determined not only by pigment conformation [since pigments with similar conformations (from UV–VIS spectroscopy) *i.e.* MBR (n = 1) *vs.* (n = 2), *vs.* (n = 3), or (n = 4) *vs.* (n = 5), show very different degrees of enantioselectivity (deduced from CD spectroscopy)], but also by the acid chain length. In this model, the MBR (n = 1) and (n = 5) pigments, with different conformations, would fit the protein highest affinity binding site with a high preference for their *P*-chirality conformation. In contrast, the MBR (n = 3) pigment, with a similar conformation as (n = 1), would fit the protein binding site with a low preference for the *M* conformation. For the rest of the pigments, covering a range of conformations, apparently the chain-length requirements for good fitting of one specific conformational enantiomer into the protein binding site are less well met: the MBR (n = 2) expectedly shows an enantioselectivity for the *P*-conformation intermediate between the high enantioselectivity of the *P*-MBR (n = 1) analogue and the low enantioselectivity of the *M*-MBR (n = 3) analogues; similarly, the pentanoic acid chain (n = 4) shows an enantioselectivity for the *P*-conformation intermediate between the low enantioselectivity of the *M*-MBR (n = 3) analogue and the high enantioselectivity of the *P*-MBR (n = 5) analogue. The situation for the (n = 7) and (n = 10) analogues is less clear. In one interpretation, the octanoic and undecanoic acid chains are sufficiently long—and flexible—to allow for a good fitting into the protein binding site by both *P* and *M* conformational enantiomers, leading to the observed lower ICD $\Delta\Delta\varepsilon$ values; *i.e.* to lower enantioselectivities by the protein.

Effect of the percentage of DMSO used as carrier

When the percentage of DMSO used as carrier to prepare the mesobilirubin-XIIIα (n = 3) HSA complex is increased from the usual 1% to *ca.* 30%, the UV–VIS spectra (compare Tables 1 and 3) remain essentially unaltered, suggesting a similar, ridge-tile type of conformation under both conditions. In contrast, the magnitude of the ICD Cotton effects increases by *ca.* 6 times, although the signed order of the Cotton effects is maintained.

In general, the changes observed as the percentage of DMSO is increased are different for each member of the series, but there appears to be no clear trend in the CD data as the alka-

Table 3 Relevant UV–VIS and induced circular dichroism spectral data[a] in pH 7.5 aqueous Tris buffer[b] for the (1:2) pigment–HSA complexes[c] of (n = 2), (n = 3), (n = 7) and (n = 10) mesobilirubin-XIIIα analogues and etiobilirubin-IVγ at 22 °C using a 30% (v/v) DMSO as carrier

	CD		UV–VIS
Mesobilirubin-XIIIα	$\Delta\varepsilon_{max}$ (λ)	λ at $\Delta\varepsilon = 0$	ε_{max} (λ)
(n = 2)	+14 (434), +5.8 (369)	—	53 600 (430)
(n = 3)	+97 (433), +89 (388)[d]	407	42 500 (434), 37 500 (408)[sh]
(n = 7)	+11 (433), −12 (398)	420	19 000 (436), 20 000 (395)
(n = 10)	+32.6 (449), −46.8 (396)[e]	—	42 000 (450), 29 000 (389)[sh]
Etiobilirubin-IVγ	+2.1 (438), −3.5 (388)	415	22 600 (432)[sh], 37 300 (375)

[a] $\Delta\varepsilon$ and ε in dm^3 mol^{-1} cm^{-1}; λ in nm. [b] 0.05 M Tris buffer. [c] *Ca.* 2.5 × 10^{-5} M pigment, *ca.* 5.0 × 10^{-5} M HSA. [d] Shoulder: −54 (418). [e] Shoulders: +19 (431), −43.6 (387).

Table 4 Relevant UV–VIS and induced circular dichroism spectral data[a] in pH 7.4 aqueous Tris buffer[b] for the (1:2) pigment–HSA complexes[c] of various bilirubins and mesobilirubins at 22 °C using different percentages (v/v) of DMSO as carrier

		CD		UV–VIS
Rubin	DMSO (%)	$\Delta\varepsilon_{max}$ (λ)	λ at $\Delta\varepsilon = 0$	ε_{max} (λ)
BR-IXα	3	+50 (450), −26 (401)	419	40 000 (456)
	30	+72 (450), −37 (400)	419	48 000 (452)
BR-IIIα	3	+69 (450), −51 (402)	423	43 600 (457)
	30	+58 (453), −40 (405)	425	42 800 (458)
BR-XIIIα	3	+22 (453), −8.4 (395)	415	27 300 (456)
	30	+39 (449), −15 (399)	416	23 100 (450)
MBR-IXα	3	+24 (430), −16 (385)	403	38 600 (433)
	30	+16 (429), −6.1 (384)	402	33 500 (429)
MBR-IIIα[d]	3	+26 (431), −27 (385)	405	27 400 (437)
	30	+58 (431), −40 (385)	407	41 400 (432)
MBR-XIIIα	3	+49 (435), −41 (390)	407	49 600 (436)
	30	+14 (434), +5.8 (369)	—	53 600 (430)

[a] $\Delta\varepsilon$ and ε in dm^3 mol^{-1} cm^{-1}. λ in nm. [b] 0.05 M Tris buffer. [c] *Ca.* 2.5 × 10^{-5} M pigment, *ca.* 5.0 × 10^{-5} M HSA. [d] Sample 90% pure, by HPLC.

noic acid chain lengthens. The MBR (n = 3) analogue has the largest negative CD Cotton effect so far, the (n = 2) complex shows a CD with two positive peaks, the (n = 7) is relatively unchanged, with its UV–VIS data still more like the alkyl analogue data and the (n = 10) shows the second largest difference in $\Delta\Delta\varepsilon$ in going from 5 to 30% DMSO. The important changes in ICD with increasing percentage of DMSO shown by the MBR (n = 3) [but also (n = 2) and (n = 10)] complexes have been interpreted above in terms of the contributions in each case by several spectroscopically different species, either the *P*-pigment HSA and *M*-pigment HSA complexes or aggregates. Indeed, a closer look at the ICD of the HSA complex of mesobilirubin (n = 3) (in 1% DMSO, Fig. 4) shows that the spectrum is composed of several partially overlapping bands, which might correspond to the sum of spectra due to different species. This is in agreement with the observation that the signed order of the ICD Cotton effects is maintained.

More generally, the changes in CD might be due to some modification in the protein's tertiary structure in 30% DMSO which could alter the shape of the binding site. However, this hypothesis is in conflict with the experimental results obtained with other, more common, bilirubin pigments. It is known, for instance, that the ICD spectra of BR-IXα HSA complexes in DMSO–water mixtures of varying composition are essentially identical.[30]

We have extended these solvent dependent CD studies to the symmetrical isomers of bilirubin; *i.e.* bilirubin-IIIα and bilirubin-XIIIα and to their meso (*i.e.* vinyl groups replaced by ethyl groups) derivatives (see formulae). The results are summarized in Table 4. Bilirubin-IIIα and bilirubin-XIIIα behave essentially as bilirubin-IXα, with CD intensities only slightly larger in 30% DMSO for the XIIIα isomer but in 3% DMSO for bilirubin-IIIα.

Interestingly, the invariability of CD spectra with percentage of DMSO seen in the vinyl bilirubins breaks down in their ethyl analogues (Table 4) and, in particular, in the XIIIα isomer. Qualitatively similar UV–VIS and CD spectral characteristics are predicted for bilirubins and mesobilirubins except with all wavelengths blue-shifted by *ca.* 25 nm in the mesobilirubins due to the substitution of the vinyl groups located in the lactam rings by ethyl groups. Apparently, it is the presence of the ethyl groups in the 3 and 17 positions that is required for the observed important change in CD with percentage of DMSO. This cosolvent might change the shape of the binding site in such a way that the greatest effect is upon the (n = 3) and perhaps also (n = 2) and (n = 10) mesobilirubin complexes (Tables 1 and 3). In this respect, the large negative CD CE found for MBR (n = 3) in 30% DMSO could indicate that the topology of HSA in 30% DMSO is optimal for binding the *M*-helical (n = 3) conformer.

This trend ends with the MBR (n = 7) complex for which the percentage of DMSO has little effect on CD and UV–VIS spectra. Also the alkyl analogue etiobilirubin-IVγ has about the same CD and UV–VIS data in 3% and 30% DMSO.

Effect of buffer

In order to determine the possible role of buffer in the spectroscopic behaviour of the mesobilirubin HSA complexes, two different buffers at pH *ca.* 7.4 were used: Trizma and phosphate. The results with Trizma (Table 1) have already been discussed. The relevant UV–VIS and CD data of the MBR (n = 2), (n = 3) and (n = 7) complexes to HSA in aqueous phosphate are summarized in Table 5.

In the CD, all the analogues show the same signed Cotton effects, except MBR (n = 3), mainly differing in intensity. The MBR (n = 3) curve is more similar to the (n = 2) than it was in Trizma, indicating that the corresponding *M*/HSA and *P*/HSA complexes are more alike here.

Concluding remarks

When bound to the highest affinity binding site of HSA, the (n = 1) to (n = 3), mesobilirubin-XIIIα analogues adopt conformations which do not differ much from the ridge-tile conformation characteristic of the BR-IXα-HSA complex. The (n = 7) and (n = 10) analogues also adopt similar conform-

Table 5 Relevant UV–VIS and induced circular dichroism spectral data[a] in pH 7.4 aqueous phosphate[b] for the (1 : 2) pigment–HSA complexes[c] of (n = 2), (n =3) and (n = 7) mesobilirubin-XIIIα analogues and etiobilirubin-IVγ at 22 °C using a 3% (v/v) DMSO as carrier[c,d]

	CD		UV–VIS
Mesobilirubin-XIIIα	$\Delta\varepsilon_{max}$ (λ)	λ at $\Delta\varepsilon = 0$	ε_{max} (λ)
(n = 2)	+35 (438), −25 (391)	408	49 800 (435)
(n = 3)	+16 (445), −23 (399)[e]	431, 378	49 600 (436)
(n = 7)	+30 (444), −39 (394)	416	19 200 (444), 16 900 (408)[sh]
Etiobilirubin-IVγ	+4.1 (436), −5.8 (389)	411	24 800 (435), 32 600 (379)[sh]

[a] $\Delta\varepsilon$ and ε in dm^3 mol^{-1} cm^{-1}; λ in nm. [b] 0.05 M phosphate buffer. [c] *Ca.* 2.5 × 10^{-5} M pigment, *ca.* 5.0 × 10^{-5} M HSA. [d] For comparable data in pH 7.4 aqueous Tris buffer [in 1% DMSO, except MBR (n = 7) in 3% DMSO], see Table 1. [e] Shoulder: +5 (360).

ations. All of these are characterized by the two dipyrrinone units folded with an angle between their dipole moments not too far from 90°; the pigments with these conformations show two maxima of comparable intensity in their UV–VIS spectra. In contrast, the conformations of the (n = 4) and (n = 5) mesobilirubins are more extended, characterized by a more symmetric, red-shifted band in the UV–VIS.

Within each group, enantioselectivity by the protein depends on acid chain length and can be inferred from the $\Delta\Delta\varepsilon$ values observed in the corresponding CD spectra. The MBR (n = 1) and (n = 5) analogues have the precise length for most effective enantioselection of the right-handed conformational enantiomer, while MBR (n = 3) apparently allows for a slight preference by the protein for the left-handed chirality pigment. In the rest of pigments, chain length allows for some effective binding of the two oppositely signed conformational enantiomers, with enantioselection of the right-handed conformation of the pigment preferred to an intermediate degree for the (n = 2) analogue and to a lower degree for the MBR (n = 4), (n = 7) and (n = 10) analogues.

Acknowledgements

We thank Dr J. Chiefari for the UV–VIS and CD data on the (n = 10) mesobilirubin-XIIIα analogue and Dr G. Puzicha for preliminary studies of albumin-induced CD spectra of many of the mesobilirubins of this study. We also thank the National Institutes of Health (HD-17779) for generous support of this work and a NATO grant (No. CRG.950626) which made this collaborative effort possible. R. V. P. gratefully acknowledges awards of an R. C. Fuson Graduate Fellowship and a Jerry and Betty Wilson Graduate Fellowship.

References

1 D. A. Lightner and A. F. McDonagh, *Acc. Chem. Res.*, 1984, **17**, 417.
2 (*a*) R. V. Person, B. R. Peterson and D. A. Lightner, *J. Am. Chem. Soc.*, 1994, **116**, 42; (*b*) R. V. Person, PhD Dissertation (Conformational Analysis of Bilirubin and its Analogues), University of Nevada, 1993.
3 P. Manitto and D. Monti, *J. Chem. Soc., Chem. Commun.*, 1976, 122.
4 G. Navon, S. Frank and D. Kaplan, *J. Chem. Soc., Perkin Trans. 2*, 1984, 1145.
5 (*a*) R. Bonnett, J. E. Davies, N. B. Hursthouse and G. M. Sheldrick, *Proc. R. Soc. London, Ser. B*, 1978, **202**, 249; (*b*) G. LeBas, A. Allegret, Y. Mauguen, C. DeRango and M. Bailly, *Acta Crystallogr., Sect. B*, 1980, **36**, 3007.
6 R. Brodersen, in *Bile Pigments and Jaundice*, ed. J. D. Ostrow, Marcel Dekker, New York, 1986; and references therein.
7 G. Blauer, E. Lavie and J. Silfen, *Arch. Biochem. Biophys.*, 1977, **492**, 64.
8 For recent reviews, see: *Pathobiology of Bilirubin and Jaundice*, in J. L. Gollan, (Guest Ed.) *Seminars in Liver Disease*, Thieme Medical Publishers, Inc., New York, 1988, vol. 8, parts 2 and 3.
9 A. F. McDonagh and D. A. Lightner, *Pediatrics*, 1985, **75**, 443.
10 A. F. McDonagh, in *The Porphyrins*, ed. D. Dolphin, Academic Press, New York, 1979, vol. VI, p. 293.
11 *Bilirubin*, eds. K. P. M. Heirwegh and S. B. Brown, CRC Press, Boca Raton, FL, 1982, vols. 1 and 2 and references therein.
12 D. A. Lightner, J. K. Gawronski and W. M. D. Wijekoon, *J. Am. Chem. Soc.*, 1987, **109**, 6354.
13 D. A. Lightner, M. Reisinger and G. L. Landen, *J. Biol. Chem.*, 1986, **261**, 6034, and references therein.
14 D. A. Lightner, W. M. D. Wijekoon and M.-H. Zhang, *J. Biol. Chem.*, 1988, **263**, 16669.
15 G. Puzicha, Y.-M. Pu and D. A. Lightner, *J. Am. Chem. Soc.*, 1991, **113**, 3583.
16 (*a*) G. Blauer, D. Harmatz and J. Snir, *Biochim. Biophys. Acta*, 1972, **278**, 68; (*b*) G. Blauer and D. Harmatz, *Biochim. Biophys. Acta*, 1972, **278**, 89; (*c*) D. Harmatz and G. Blauer, *Arch. Biochem. Biophys.*, 1975, **170**, 375; (*d*) G. Blauer and G. Wagnière, *J. Am. Chem. Soc.*, 1975, **97**, 1949; (*e*) G. Blauer, *Isr. J. Chem.*, 1983, **23**, 201.
17 J. Jacobsen and R. Brodersen, *J. Biol. Chem.*, 1983, **258**, 6319.
18 J. Broos, A. J. W. G. Visser, J. F. J. Engbersen, W. Verboom, A. van Hock and D. N. Reinhoudt, *J. Am. Chem. Soc.*, 1995, **117**, 12657.
19 H. Murakawa, J. Abe, A. Seki and H. Takahashi, *J. Mol. Struct.*, 1993, **297**, 41.
20 F. R. Trull, D. P. Shrout and D. A. Lightner, *Tetrahedron*, 1992, **48**, 8189.
21 J.-S. Ma and D. A. Lightner, *J. Heterocycl. Chem.*, 1984, **21**, 1005.
22 M. Fontich, M. Rodríguez and F. R. Trull, *Synth. Commun.*, 1994, **24**, 993.
23 M. Reisinger, F. R. Trull and D. A. Lightner, *J. Heterocycl. Chem.*, 1985, **22**, 1221.
24 F. R. Trull, M. Rodríguez and D. A. Lightner, *Synth. Commun.*, 1993, **23**, 2771.
25 F. R. Trull, R. W. Franklin and D. A. Lightner, *J. Heterocycl. Chem.*, 1987, **24**, 1573.
26 D. P. Shrout, G. Puzicha and D. A. Lightner, *Synthesis*, 1992, **3**, 328.
27 J. Chiefari, R. V. Person and D. A. Lightner, *Tetrahedron*, 1992, **48**, 5969.
28 W. L. Shelver, H. Rosenberg and W. H. Shelver, *Int. J. Quantum Chem.*, 1992, **44**, 141.
29 D. A. Lightner, R. V. Person, B. R. Peterson, G. Puzicha, Y.-M. Pu and S. E. Bojadziev, *Biomolecular Spectroscopy II*, eds. R. R. Birge and L. A. Nafie, Proc. SPIE, 1991, **1432**, 2.
30 R. V. Person, S. E. Boiadjiev, B. R. Peterson, G. Puzicha and D. A. Lightner, *4th International Conference on Circular Dichroism*, Sept. 9–13, 1991, Bochum, FRG, p. 55.
31 M. Kasha, H. R. Rawls and M. A. El-Bayoumi, *Pure Appl. Chem.*, 1965, **32**, 371.
32 N. Harada and K. Nakanishi, *Circular Dichroic Spectroscopy-Exciton Coupling in Organic Stereochemistry*, University Science Books, Mill Valley, CA, 1983.
33 Data from reverse-phase HPLC column using a 0.1 M di-octylammonium acetate in MeOH buffer with 5% water at pH 7.7 according to A. F. McDonagh, L. A. Palma, F. R. Trull and D. A. Lightner, *J. Am. Chem. Soc.*, 1982, **104**, 6865.
34 S. E. Boiadjiev, R. V. Person, G. Puzicha, C. Knobler, E. Maverick, K. N. Trueblood and D. A. Lightner, *J. Am. Chem. Soc.*, 1992, **114**, 10123.
35 Y.-M. Pu, A. F. McDonagh and D. A. Lightner, *J. Am. Chem. Soc.*, 1993, **115**, 377.
36 H. Falk, T. Schlederer and P. Wolschann, *Monatsch Chem.*, 1981, **112**, 199.

Paper 6/04897H
Received 12*th July* 1996
Accepted 12*th February* 1997